EGTRIB Journal
JOURNAL OF
THE EGYPTIAN SOCIETY OF TRIBOLOGY
VOLUME 21, No. 2, April 2024, pp. 53 – 61 **ISSN 2090 - 5882**
(Received November 21. 2023, Accepted in final form February 16. 2024) **jest.journals.ekb.eg**

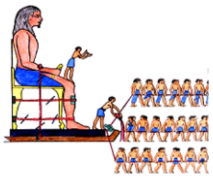

FACTORS AFFECTING THE COEFFICIENT OF FRICTION IN A DIRECT CURRENT TRIBOELECTRIC NANOGENERATOR

Rashed A., Al-Kabbany A. M., Ali W. Y. and Ameer A. K.

Department of Production Engineering and Mechanical Design, Faculty of Engineering, Minia University, Minia 61111, Egypt.

ABSTRACT
The triboelectric nanogenerator (TENG) has proved to be an important innovation in the field of self-powered sensors. It utilizes triboelectrification and electrostatic induction in order to generate power. Multiple types of TENGs exist, but one type that uses electrostatic breakdown to generate power is the sliding direct current TENG (DC-TENG) that consists of a friction electrode (FE) and a charge collecting electrode (CCE). This paper discusses the factors affecting the coefficient of friction (COF) between a DC-TENG and the triboelectric layer (TL). The tested DC-TENG had a trailing CCE that was allowed to float on the surface of the lubricating oil.

It was found that lubrication via motor oil showed the lowest values of (COF) in most cases. But for high sliding velocitys and low normal load conditions, the dry sliding condition gave the lowest values of COF. It was revealed that COF also increased with normal force in all cases except when lubricated by motor oil. The relationship between the COF and the sliding velocity of the DC-TENG was found to follow the Stribeck diagram. COF was also found to increase with load resistance due to charge accumulation on the FE.

KEYWORDS
Sliding, triboelectric nanogenerator, paraffin, motor oil.

INTRODUCTION
It is well known that charges can occasionally be transferred from one material to another if they come into contact with one another. This phenomenon is known as triboelectrification or the triboelectric effect, [1 - 3]. This effect is thought to be a result of an exchange of ions in the case of polymers and an exchange of electrons in the case of metals, [4], the likelihood of materials to obtain a positive charge when they touch another material is ranked by the triboelectric series, [5 - 7].

The triboelectric effect was used in conjunction with electrostatic induction in order to generate energy. The device that does that is called a triboelectric nanogenerator

(TENG), [8, 9]. TENGs can be used in energy harvesting, [10 - 12] and in making self-powered sensors, [13 - 16]. It also has many types, such as contact-separation mode TENGs, [17 - 19], sliding mode TENGs, [20 - 22], single electrode TENGs, [23 - 26], and freestanding mode TENGs, [27 - 29].
Sliding mode TENGs can be classified into two types. AC sliding mode TENGs and DC sliding mode TENGs (DC-TENG). AC sliding mode TENGs work via electrostatic induction and triboelectrification. DC-TENGs work via triboelectrification and electrostatic breakdown, [30 - 32]. DC-TENGs consist of a TL on that the DC-TENG slides (usually a dielectric material). The DC-TENG consists of a friction electrode FE that slides on the TL and a charge-collecting electrode (CCE) that has a small vertical distance between itself and the TL and moves with the FE. When the FE slides on the TL, the triboelectric effect causes charges to form on the FE and the TL. The charges that formed on the TL then cause a potential difference between itself and the CCE. This causes air breakdown to occur that causes charges to accumulate on the CCE. Those charges later flow to the FE and later to the TL, completing the cycle and the moving charges create an electrical current, and thus electric power.

The use of lubrication in DC-TENGs has been proven to improve the electrical output of a DC-TENG, [33, 34]. It can also help decrease wear and provide separation between the CCE and the TL. This study investigates the effect of the contact force between the FE and the TL, the sliding velocity of the DC-TENG, and the electrical resistance between the CCE and the FE on COF between a DC-TENG with an aluminum foil FE and a Kapton TL.

EXPERIMENTAL

A DC-TENG was prepared using a $30 \times 30 \times 3$ mm^3 polymethylmethacrylate (PMMA) substrate. Attached to the bottom of said substrate is an FE made from 0.1 mm thick aluminum film on top of a piece of 800 grit sandpaper. Attached vertically to the PMMA substrate was a metal rod wrapped in polytetrafluoroethylene (PTFE) film. This rod was fastened to the moving part of a power screw-driven device that can transport the TENG in a straight line, Fig. 1. Attached to the PMMA substrate via Kapton tape was another 30×20 mm^2 PMMA substrate and 10 mm behind the FE. Fastened to this substrate was a CCE made from the same aluminum foil-sandpaper structure as the FE. No vertical weight was applied on the CCE. This DC-TENG was tested on a 0.1 mm thick Kapton TL attached to a wooden substrate. Lubricant was also applied to the TL, Fig. 2.

The device shown in Fig. 1 has a load cell attached to its moving part. This load cell can be used to measure the friction force as the DC-TENG moves. The load cell was attached to an HX711 chip attached to an Arduino Nano that was used to monitor the friction force. The effect of three different parameters on the coefficient of friction between the TL and the DC-TENG was investigated. The first parameter was the normal force applied on the DC-TENG, the second was the sliding velocity and the third was the electrical resistance between the CCE and the FE. Each test was repeated for three different lubrication conditions: lubrication by paraffin oil, motor oil, and dry sliding. The normal force range tested was from 4 N to 12 N (with open-

circuit (OC) condition and a sliding velocity of 2.5 cm/s), the sliding velocity range was from 1.27 to 2.5 cm/s under OC condition and a normal force of 4 N, and the resistance range was from 1 Ω to 10 MΩ (with a sliding velocity of 2.5 cm/s and a normal force of 4 N).

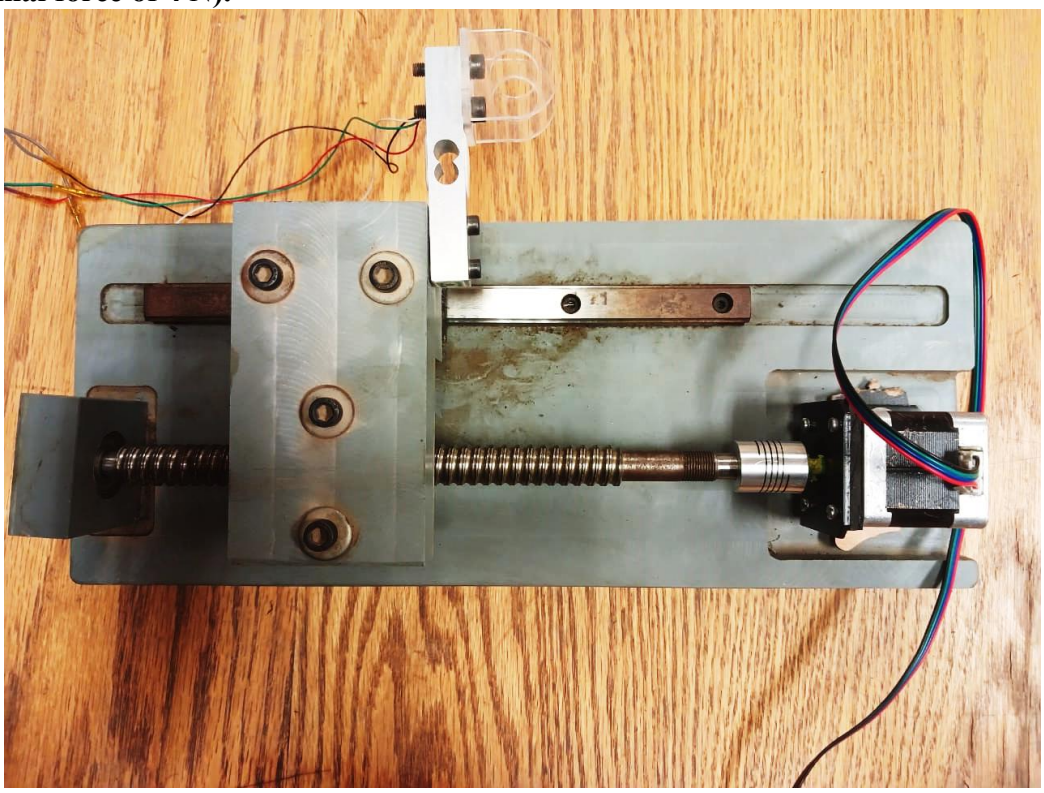

Fig. 1 The power screw-driven test device.

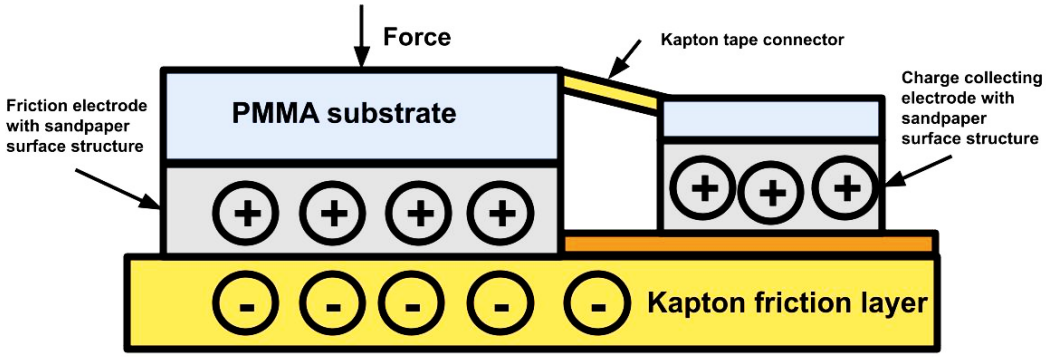

Fig. 2 The tested DC-TENG.

RESULTS AND DISCUSSION

Data of friction force versus time were collected for every test condition. The COF between the TENG and the TL can be obtained when the friction force is divided by the normal force. The nature of the COF versus time relationship for each test can be seen in the example shown in Fig. 3. COF rises quickly until it reaches the static COF value for the system. Once the TENG starts moving, the COF starts to decrease due to the dynamic COF being lower than the static COF value.

The values of the COF versus contact force showed that COF decreased with load only in the case of the motor oil condition, while increasing with load in the case of both the paraffin and the dry conditions as shown in fig. 4. The dry condition showed the lowest values of COF at normal loads lower than 8 N, while lubricating the FS with the motor oil showed the lowest values of COF at higher normal loads. The reason the COF increased with the load could be due to the interlocking of asperities on both the FE and the TL causing an increase in the friction force at higher normal loads. The decrease in COF with load in the case of motor oil is probably due to anti-wear additives that were added to the oil causing the friction force to stay relatively stable at different loads. Thus, decreasing the COF.

The COF also decreased with an increase in sliding velocity as shown in Fig. 5. Being the lowest in the case of lubrication by motor oil. This is thought to be due to the hydrodynamic effect causing more separation between the TL and the FE as the sliding velocity increases. This follows the expected relationship between COF and sliding velocity (Stribeck diagram). Where due to the hydrodynamic effect, the lubrication mode changes from boundary all the way up to hydrodynamic lubrication. In this relationship, COF decreases with sliding velocity until the lubrication mode reaches elasto-hydrodynamic lubrication.

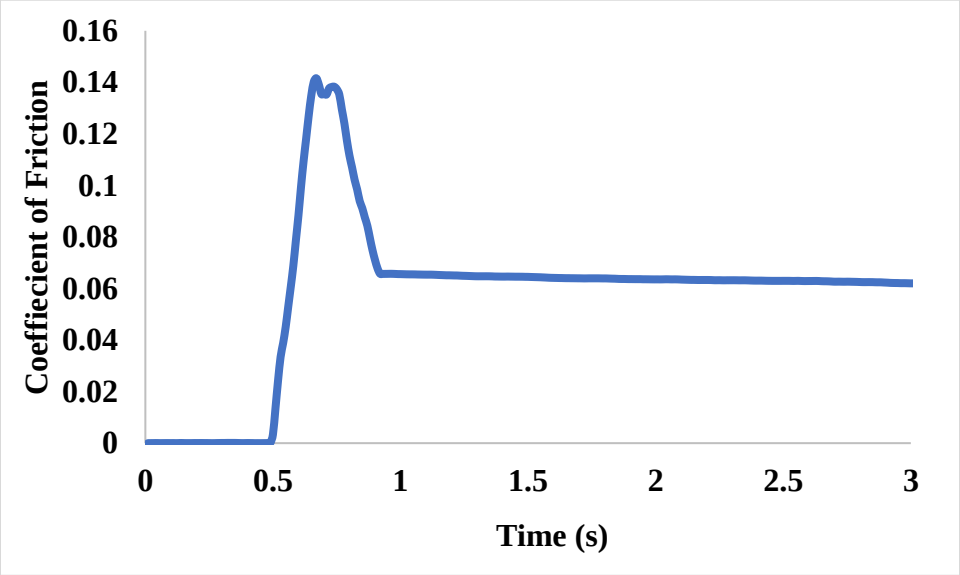

Fig. 3 Example of a COF measurement curve under 4 N normal force and oil lubrication.

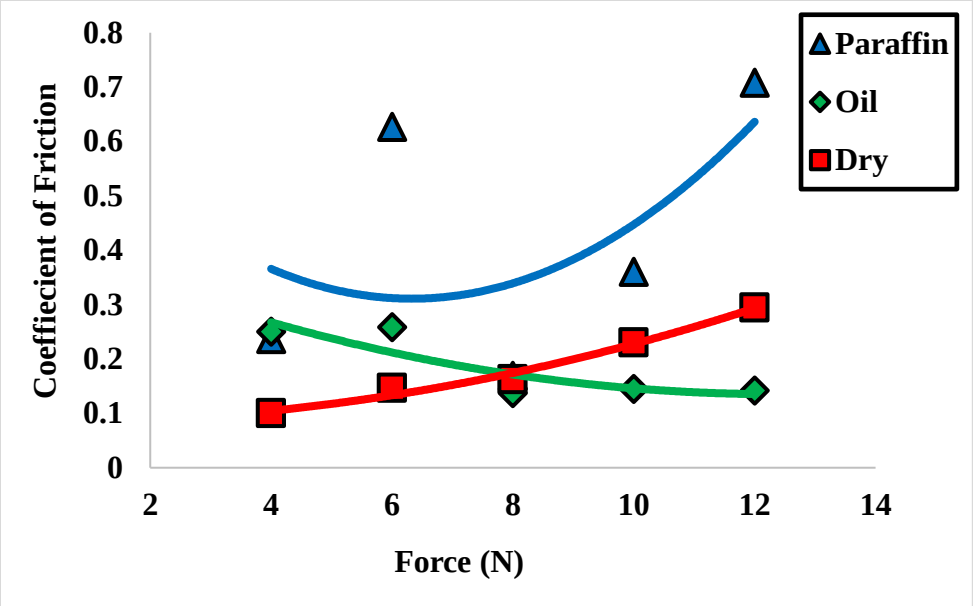

Fig. 4 COF versus contact force for each test condition.

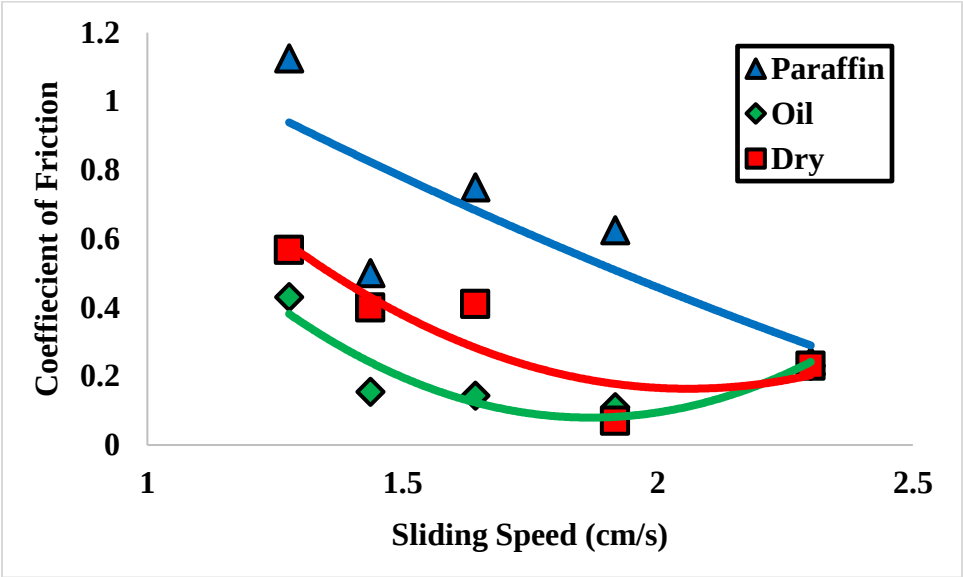

Fig. 5 COF versus sliding velocity for each test condition.

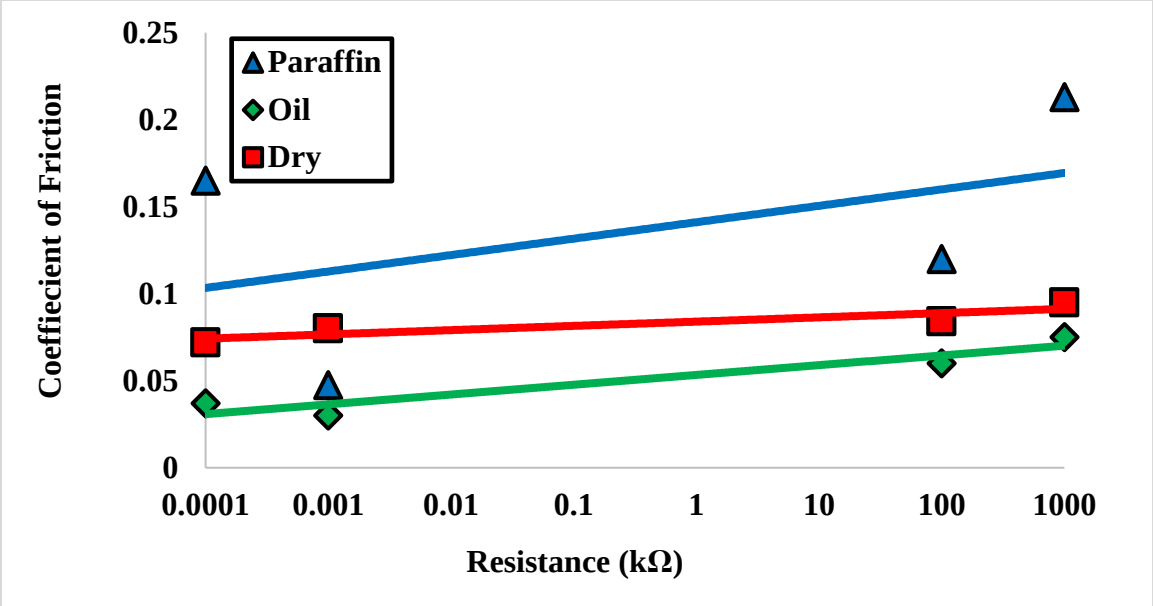

Fig. 6 COF vs load resistance for each test condition (logarithmic scale).

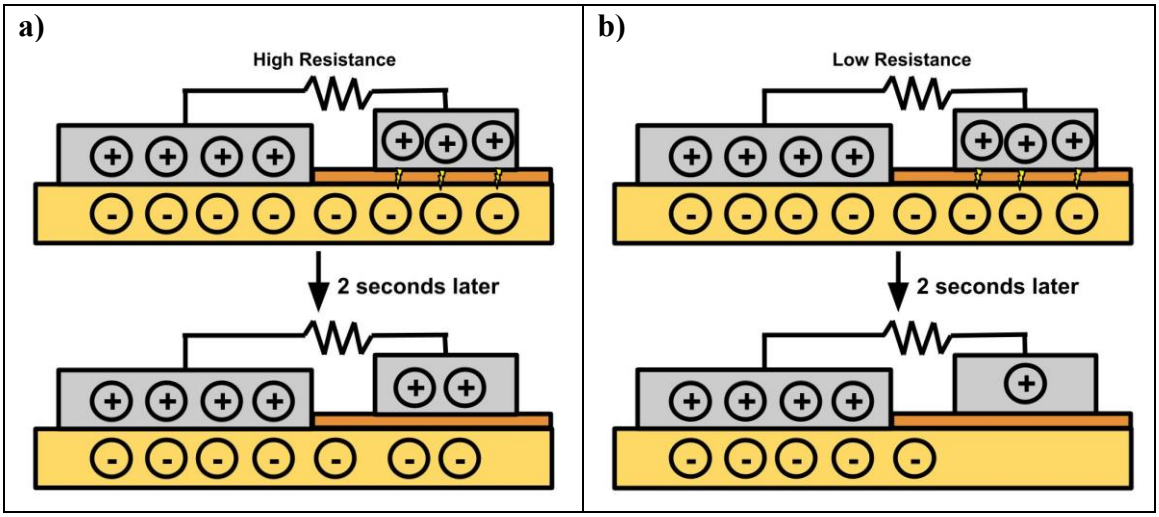

Fig. 7. Charge accumulation on the CCE in different cases: a) High resistance case. b) Low resistance case.

COF seemed to increase as the load resistance increased in all the three lubrication conditions as shown in Fig. 6. The lowest values were observed in the case of lubrication via motor oil as well. A possible explanation for this phenomenon can be an accumulation of charges on the CCE as the DC-TENG moves. Since TENGs are usually equated to capacitors in electric circuits, this means that an increase in the load resistance increases the time constant of the circuit. This causes charges to accumulate on the FE at high resistances as the TENG moves on the TL rather than moving on the CCE and going back to the TL. This accumulated charge can cause an increased attraction force between the FE and the TL that increases the COF, Fig. 7.

CONCLUSIONS

1. Motor oil provided the lowest values of COF in most cases.
2. At high velocities and low normal loads, dry sliding gave the lowest values of COF.
3. COF mostly increased with normal load, except in the case of motor oil where it decreased with normal load. Probably due to anti-wear additives.
4. The relationship between COF and sliding velocity followed the Stribeck behavior.
5. Increasing the load resistance increases the COF, due to charges accumulated on the FE causing an increased attraction between it and the TL.

REFERENCES

1. Ali A. S., Al-Kabbany A. M., Ali W. Y., and Samy A. M., "Reducing the Electrostatic Charge Generated From Sliding of Rubber on Polyethylene Artificial Turf," Journal of the Egyptian Society of Tribology, Vol. 17, No. 2, pp. 40–49, (2020), doi: 10.21608/jest.2020.81899.
2. Al-Kabbany A. M. and Ali W. Y., "Reducing The Electrostatic Charge of Polyester by Blending by Polyamide Strings," Journal of the Egyptian Society of Tribology, Vol. 16, No. 4, pp. 36–44, (2019), doi: 10.21608/jest.2019.78876.
3. Ali A. S., "Triboelectrification of Synthetic Strings," Journal of the Egyptian Society of Tribology, Vol. 16, No. 2, pp. 26–36, (2019), doi: 10.21608/JEST.2019.79377.
4. McCarty L. S. and Whitesides G. M., "Electrostatic charging due to separation of ions at interfaces: contact electrification of ionic electrets," Angewandte Chemie International Edition, Vol. 47, No. 12, pp. 2188–2207, (2008), doi: 10.1002/anie.200701812.
5. Burgo T. A. L., Galembeck F., and Pollack G. H., "Where is water in the triboelectric series?," Journal of Electrostatics, Vol. 80, pp. 30–33, (2016), doi: 10.1016/j.elstat.2016.01.002.
6. Zou H., Zhang Y., Guo L., Wang P., He X., Dai G., Zheng H., Chen C., Wang A. C., Xu C., and others, "Quantifying the triboelectric series," Nature communications, Vol. 10, No. 1, p. 1427, (2019), doi: 10.1038/s41467-019-09461-x.
7. Diaz A. F. and Felix-Navarro R. M., "A semi-quantitative tribo-electric series for polymeric materials: the influence of chemical structure and properties," Journal of Electrostatics, Vol. 62, No. 4, pp. 277–290, (2004), doi: 10.1016/j.elstat.2004.05.005.
8. Niu S. and Wang Z. L., "Theoretical systems of triboelectric nanogenerators," Nano Energy, Vol. 14, pp. 161–192, (2015).
9. Fan F.-R., Tian Z.-Q., and Lin Wang Z., "Flexible triboelectric generator," Nano Energy, Vol. 1, No. 2, pp. 328–334, (2012), doi: 10.1016/j.nanoen.2012.01.004.
10. Han J., Feng Y., Chen P., Liang X., Pang H., Jiang T., and Wang Z. L., "Wind-driven soft-contact rotary triboelectric nanogenerator based on rabbit fur with high performance and durability for smart farming," Advanced Functional Materials, Vol. 32, No. 2, p. 2108580, (2022), doi: 10.1002/adfm.202108580.
11. Niu S., Wang S., Lin L., Liu Y., Zhou Y. S., Hu Y., and Wang Z. L., "Theoretical study of contact-mode triboelectric nanogenerators as an effective power source," Energy & Environmental Science, Vol. 6, No. 12, pp. 3576–3583, (2013), doi: 10.1039/C3EE42571A.
12. Cheng P., Guo H., Wen Z., Zhang C., Yin X., Li X., Liu D., Song W., Sun X., Wang J., and others, "Largely enhanced triboelectric nanogenerator for efficient harvesting

of water wave energy by soft contacted structure," Nano Energy, Vol. 57, pp. 432–439, (2019), doi: 10.1016/j.nanoen.2018.12.054.
13. Fan F.-R., Lin L., Zhu G., Wu W., Zhang R., and Wang Z. L., "Transparent triboelectric nanogenerators and self-powered pressure sensors based on micropatterned plastic films," Nano letters, Vol. 12, No. 6, pp. 3109–3114, (2012).
14. Meng B., Tang W., Too Z., Zhang X., Han M., Liu W., and Zhang H., "A transparent single-friction-surface triboelectric generator and self-powered touch sensor," Energy & Environmental Science, Vol. 6, No. 11, pp. 3235–3240, (2013), doi: 10.1039/C3EE42311E.
15. Zhou Q., Pan J., Deng S., Xia F., and Kim T., "Triboelectric nanogenerator-based sensor systems for chemical or biological detection," Advanced Materials, Vol. 33, No. 35, p. 2008276, (2021), doi: 10.1002/adma.202008276.
16. Jin T., Sun Z., Li L., Zhang Q., Zhu M., Zhang Z., Yuan G., Chen T., Tian Y., Hou X., and others, "Triboelectric nanogenerator sensors for soft robotics aiming at digital twin applications," Nature communications, Vol. 11, No. 1, p. 5381, (2020), doi: 10.1038/s41467-020-19059-3.
17. Lee S. and Park Y.-B., "Contact-separation mode triboelectric nanogenerator utilizing carbon-fiber composite structure for harvesting mechanical energy," Funct. Compos. Struct, Vol. 5, p. 35007, (2023), doi: 10.1088/2631-6331/acf124.
18. Wardhana E. M., Mutsuda H., Tanaka Y., Nakashima T., Kanehira T., Taniguchi N., Maeda S., Yonezawa T., and Yamauchi M., "Harvesting contact-separation-compression vibrations using a flexible and compressible triboelectric generator," Sustainable Energy Technologies and Assessments, Vol. 42, p. 100869, (Dec. 2020), doi: 10.1016/J.SETA.2020.100869.
19. Jurado U. T., Pu S. H., and White N. M., "A contact-separation mode triboelectric nanogenerator for ocean wave impact energy harvesting," Proceedings of IEEE Sensors, Vol. 2017-December, pp. 1–3, (Dec. 2017), doi: 10.1109/ICSENS.2017.8234198.
20. He W., Liu W., Chen J., Wang Z., Liu Y., Pu X., Yang H., Tang Q., Yang H., Guo H., and Hu C., "Boosting output performance of sliding mode triboelectric nanogenerator by charge space-accumulation effect," Nature Communications 2020 11:1, Vol. 11, No. 1, pp. 1–8, (Aug. 2020), doi: 10.1038/s41467-020-18086-4.
21. Zhang H., Zhang C., Zhang J., Quan L., Huang H., Jiang J., Dong S., and Luo J., "A theoretical approach for optimizing sliding-mode triboelectric nanogenerator based on multi-parameter analysis," Nano Energy, Vol. 61, pp. 442–453, (Jul. 2019), doi: 10.1016/J.NANOEN.2019.04.057.
22. Niu S., Liu Y., Wang S., Lin L., Sheng Zhou Y., Hu Y., Lin Wang Z., Niu S., Liu Y., Wang S., Lin L., Zhou Y. S., Hu Y., and Wang Z. L., "Theory of Sliding-Mode Triboelectric Nanogenerators," Advanced Materials, Vol. 25, No. 43, pp. 6184–6193, (Nov. 2013), doi: 10.1002/ADMA.201302808.
23. Su Y., Yang Y., Zhong X., Zhang H., Wu Z., Jiang Y., and Wang Z. L., "Fully enclosed cylindrical single-electrode-based triboelectric nanogenerator," ACS Applied Materials and Interfaces, Vol. 6, No. 1, pp. 553–559, (Jan. 2014), doi: 10.1021/AM404611H/SUPPL_FILE/AM404611H_SI_001.PDF.
24. Zhang H., Yang Y., Zhong X., Su Y., Zhou Y., Hu C., and Wang Z. L., "Single-electrode-based rotating triboelectric nanogenerator for harvesting energy from

tires," ACS Nano, Vol. 8, No. 1, pp. 680–689, (Jan. 2014), doi: 10.1021/NN4053292 /SUPPL_FILE/NN4053292_SI_004.AVI.
25. Niu S., Liu Y., Wang S., Lin L., Zhou Y. S., Hu Y., and Wang Z. L., "Theoretical Investigation and Structural Optimization of Single-Electrode Triboelectric Nanogenerators," Advanced Functional Materials, Vol. 24, No. 22, pp. 3332–3340, (Jun. 2014), doi: 10.1002/ADFM.201303799.
26. Mao Y., Geng D., Liang E., and Wang X., "Single-electrode triboelectric nanogenerator for scavenging friction energy from rolling tires," Nano Energy, Vol. 15, pp. 227–234, (Jul. 2015), doi: 10.1016/J.NANOEN.2015.04.026.
27. Jiang T., Chen X., Han C. B., Tang W., Wang Z. L., Jiang T., Chen X., Han C. B., Tang W., and Wang Z. L., "Theoretical Study of Rotary Freestanding Triboelectric Nanogenerators," Advanced Functional Materials, Vol. 25, No. 19, pp. 2928–2938, (May 2015), doi: 10.1002/ADFM.201500447.
28. Niu S., Liu Y., Chen X., Wang S., Zhou Y. S., Lin L., Xie Y., and Wang Z. L., "Theory of freestanding triboelectric-layer-based nanogenerators," Nano Energy, Vol. 12, pp. 760–774, (Mar. 2015), doi: 10.1016/J.NANOEN.2015.01.013.
29. Chen Y., Wang P., Wang C., Li J., Tan M., and Zhao M., "Design of bubble-based plasma sterilization system based on freestanding rotary triboelectric nanogenerator," Materials Today Sustainability, Vol. 24, p. 100606, (Dec. 2023), doi: 10.1016/J.MTSUST.2023.100606.
30. Song Y., Wang N., Wang Y., Zhang R., Olin H., Yang Y., Song Y., Wang N., Yang Y., Wang Y., Zhang R., and Olin H., "Direct Current Triboelectric Nanogenerators," Advanced Energy Materials, Vol. 10, No. 45, p. 2002756, (Dec. 2020), doi: 10.1002/AENM.202002756.
31. Liang S., Li C., Niu M., Naval S., Jain A., and Mallick D., "Direct current triboelectric nanogenerators: a review," Journal of Micromechanics and Microengineering, Vol. 33, No. 1, p. 013001, (Dec. 2022), doi: 10.1088/1361-6439/ACA59E.
32. Song W. Z., Qiu H. J., Zhang J., Yu M., Ramakrishna S., Wang Z. L., and Long Y. Z., "Sliding mode direct current triboelectric nanogenerators," Nano Energy, Vol. 90, p. 106531, (Dec. 2021), doi: 10.1016/J.NANOEN.2021.106531.
33. Zhou L., Liu D., Zhao Z., Li S., Liu Y., Liu L., Gao Y., Wang Z. L., and Wang J., "Simultaneously Enhancing Power Density and Durability of Sliding-Mode Triboelectric Nanogenerator via Interface Liquid Lubrication," Advanced Energy Materials, Vol. 10, No. 45, p. 2002920, (Dec. 2020), doi: 10.1002/AENM.202002920.
34. Qiao W., Zhao Z., Zhou L., Liu D., Li S., Yang P., Li X., Liu J., Wang J., and Wang Z. L., "Simultaneously Enhancing Direct-Current Density and Lifetime of Tribovotaic Nanogenerator via Interface Lubrication," Advanced Functional Materials, Vol. 32, No. 46, (Nov. 2022), doi: 10.1002/adfm.202208544.